# "Decoration" of Shell Cross-Linked Reverse Polymer Micelles Using ATRP: A New Route to Stimuli-Responsive Nanoparticles

**Jérôme Babin,† Martin Lepage,*,‡ and Yue Zhao*,†**

*Département de chimie and Département de médecine nucléaire et de radiobiologie and Centre d'imagerie moléculaire de Sherbrooke, Université de Sherbrooke, Sherbrooke, Québec, Canada J1K 2R1*

*Received October 31, 2007; Revised Manuscript Received December 13, 2007*

ABSTRACT: We demonstrate the use of atom transfer radical polymerization (ATRP) to graft polymers onto preformed shell cross-linked reverse micelles (SCRM). Reverse polymer micelles are first obtained in organic solvents and stabilized by cross-linking of the shell using the photoinduced dimerization of coumarin groups (>310 nm). The structurally locked SCRM are then used as micellar macroinitiators for further polymerization from their surface of monomers such as styrene and dimethylaminoethyl methacrylate (DMAEMA) via ATRP. The decoration of an outer corona of PDMAEMA renders the nanoparticles containing a hydrophilic core soluble in water, with the solubility being sensitive to changes in pH and temperature. In addition, such decorated SCRM are light-responsive. The photoinduced cleavage of cyclobutane bridges (<260 nm) leads to the de-cross-linking of the shell and thus the disintegration of the micellar aggregates. The characterization results, using size-exclusion chromatography (SEC), dynamic light scattering (DLS), and transmission electron microscope (TEM), show an excellent control over the reactions, the molar mass, and the polydispersity of SCRM before and after the surface-initiated ATRP. The "decoration" of SCRM offers a new route to designing stimuli-responsive polymer nanostructures that cannot be prepared through only block copolymer self-assembly.

## Introduction

Surface-initiated atom transfer radical polymerization (ATRP) has been widely exploited for surface modifications or functionalization.[1,2] Generally, catalyzed by a transition metal complex, the presence of halide groups on a variety of surfaces allows for the ATRP of a chosen monomer, and the resulting polymer can modify the properties of or impart new functions to the surface. Of particular interest is the use of surface-initiated ATRP to decorate nanoscale materials such as inorganic nanoparticles.[3−6] This approach can be adapted to many other systems. To name only a few examples, Gnanou et al. prepared amphiphilic dendrimer-like architectures by growing polystyrene (PS) from poly(ethylene oxide) (PEO) stars.[7] Couet and Biesalski obtained self-assembled cyclic peptide nanotubes wrapped in a polymer by using the nanotube surface-initiated ATRP of *N*-isopropylacrylamide.[8] Advincula's group reported the synthesis of colloidal particles coated first with layer-by-layer (LBL) assembled polyelectrolytes and then with polymer grafts grown on the surface of the LBL film containing the initiator groups.[9]

Another subject of interest is the stabilization of self-assembled block copolymer core−shell micelles to ensure their structural integrity in a certain range of temperature, concentration, pH or in the presence of organic solvents.[10,11] Wooley's group described the shell cross-linking of polystyrene-*b*-poly(4-vinylpyridine) (PS-*b*-PVP)-based micelles by a radical process in the presence of an external photoinitiator[12] and of polystyrene-*b*-poly(acrylic acid) micelles by amidation using a diamino linker.[13] Liu et al. took a different approach based on the use of photochemically self-cross-linkable monomer of 2-cinnamoylethyl methacrylate.[14,15] However, one limiting aspect in these strategies is the lack of reversibility. A method allowing the reversibility was reported by Kataoka et al.[16] They showed that stabilized polyion complex micelles can be obtained by cross-linking the core through disulfide bonds and, subsequently, dissociated by cleaving the disulfide bond with a reducing reagent. A similar approach based on the thiol/disulfide exchange has also been proposed for the synthesis of reversible shell cross-linked micelles.[17]

The purpose of the present work was to investigate the use of surface-initiated ATRP to decorate preformed and stabilized polymer micelles, which are a nanoscale system of considerable interest. The strategy we used is depicted in Figure 1. We started with an amphiphilic diblock copolymer of poly(dimethylaminoethyl methacrylate)$_{54}$-*block*-poly(methyl methacrylate$_{55}$-*random*-coumarin methacrylate$_{19}$) [PDMAEMA$_{54}$-*b*-P(MMA$_{55}$-*co*-CMA$_{19}$)]. As this diblock was synthesized using ATRP with chlorine-terminated PDMAEMA$_{54}$ macroinitiator, the halide initiator groups were transferred to the chain ends of the hydrophobic P(MMA$_{55}$-*co*-CMA$_{19}$) random copolymer. Obviously, to initiate ATRP from the micelle surface, the halide groups need to be exposed on the surface (or close to the surface) of the micelles. This is why reverse polymer micelles with neutralized (hydrophilic) PDMAEMA$_{54}$ core and P(MMA$_{55}$-*co*-CMA$_{19}$) shell were prepared in a low-polarity solvent (mixture of THF/dichloromethane). And considering that a subsequent ATRP using the micellar macroinitiator demands the structural integrity of the reverse micelles in the solvent that is suitable for the polymerization of the chosen monomer, the micelle shell was photo-cross-linked through the dimerization of the coumarin side groups on the P(MMA$_{55}$-*co*-CMA$_{19}$) blocks upon UV irradiation at $\lambda > 310$ nm.[18] An attractive feature with the use of coumarin moieties is that the cyclobutane bridges resulting from the dimerization can be photocleaved upon UV irradiation at shorter wavelengths of $\lambda < 260$ nm, leading to the photo-de-cross-linking of the hydrophobic shell and the disintegration of SCRM. In this work, we used the structurally locked shell cross-linked reverse micelles (SCRM)

* Corresponding authors. E-mail: yue.zhao@usherbrooke.ca; martin.lepage@usherbrooke.ca.
† Département de chimie.
‡ Département de médecine nucléaire et de radiobiologie.

10.1021/ma702422y CCC: $40.75 
Published on Web 02/05/2008

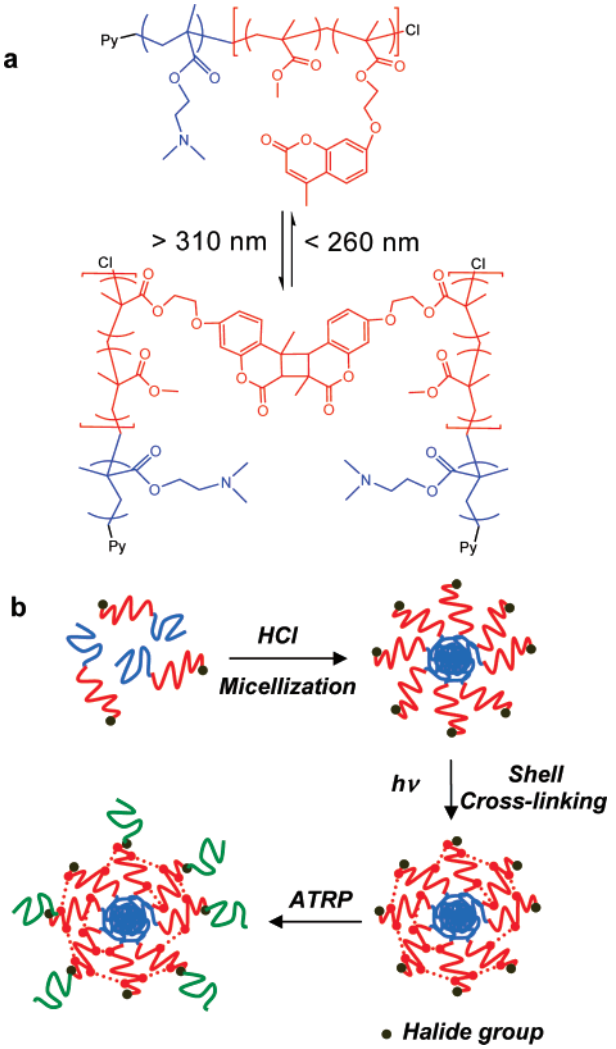


**Figure 1.** (a) UV photodimerization and photocleavage of coumarin side groups in PDMAEMA$_{54}$-*b*-P(MMA$_{55}$-*co*-CMA$_{19}$) block copolymer. (b) Illustration of the approach used to obtain and "decorate" shell cross-linked reverse micelles (SCRM) formed by the diblock copolymer.

of PDMAEMA$_{54}$-*b*-P(MMA$_{55}$-*co*-CMA$_{19}$) to initiate polymerization of styrene and dimethylaminoethyl methacrylate (DMAEMA) in DMF, giving rise to polymer nanoparticles composed of a dense hydrophilic core, a photocontrollable hydrophobic shell, and an outer grafted corona. In the case of SCRM decorated with PDMAEMA, they are soluble in water and respond to changes in pH and temperature. The interest of this work is twofold. First, it is challenging to obtain reverse polymer micelles stable in aqueous solution, thus suitable for potential delivery applications;[19] this work introduces a general strategy to do this, which is based on shell cross-linking the reverse polymer micelles followed by surface decoration of an outer water-soluble polymer corona. As mentioned above, there are many reports on shell cross-linked polymer micelles,[10−13] but shell cross-linked reverse polymer micelles are rare. Second, this work shows that combining block copolymer micellar self-assembly and post-surface-functionalization through ATRP is an interesting approach to build up more complex polymer nanostructures.

## Experimental Section

**1. Synthesis of The PDMAEMA$_{54}$-*b*-P(MMA$_{55}$-*co*-CMA$_{19}$) Diblock Copolymer. Materials.** Styrene (99%), dimethylaminoethyl methacrylate (DMAEMA, 99%), and methyl methacrylate (MMA, 98%) were passed through a basic alumina column and distilled prior to use. Tetrahydrofuran (THF, 99%) was distilled from sodium benzophenone. Triethylamine (99%) was distilled over KOH. 2-Bromo-2-methylpropionyl bromide, Nile RED (NR), 1-pyrenemethanol (98%), copper(I) chloride (CuCl, 98%), *N*,*N*′,*N*′,*N*′′-pentamethyldiethylenetriamine (PMDETA, 99%), 1,1,4,7,10,10-hexamethyltriethylenetetramine (HMTETA, 99%), anhydrous anisole, methanol, and *N*,*N*-dimethylformamide were used as received. All reagents were purchased from Aldrich. 7-(2-Methacryloyloxyethoxy)-4-methylcoumarin monomer was synthesized as described previously.[17]

**Synthesis of 1-Pyrenylmethyl 2-Bromopropanoate ATRP Initiator (Py-Br).** In a 125 mL round-bottom flask flamed and dried under vacuum, the 1-pyrenemethanol (5 g, 0.021 55 mol) was dissolved in dry THF (50 mL) along with triethylamine (3.23 g, 0.0323 mol). A solution of 2-bromo-2-methylpropionyl bromide (5.85 g, 0.025 86 mol) in THF (20 mL) was added dropwise at 0 °C over a period of 10 min. After stirring for 4 h at room temperature, the resulting insoluble amine hydrobromide salt was removed by filtration, and most of the THF solvent was removed by rotary evaporation. The residue was dissolved with dichloromethane and extracted three times with a $K_2CO_3$ water solution. The organic phase was separated, dried over magnesium sulfate, filtered, and evaporated to dryness. Finally, after recrystallization in methanol and vacuum drying, 1-pyrenylmethyl 2-bromopropanoate (Py-Br) was obtained (yield: 93%). $^1$H NMR ($CDCl_3$) $\delta$ (ppm): 8.3−8 (m, 9H aromatic), 5.9 (s, 2H, py-C$H_2$OCO), 1.9 (s, 6H, OCOC(C$H_3$)$_2$Br).

**Synthesis of Pyrene-Labeled Poly(dimethylaminoethyl methacrylate)$_{54}$ ATRP Macroinitiator (Py-PDMAEMA$_{54}$-Cl).** In a typical experiment, a round-bottom flask flamed and dried under vacuum was charged with 0.106 g ($1.07 \times 10^{-3}$ mol) of CuCl, 0.29 g ($1.07 \times 10^{-3}$ mol) of HMTETA, 9 mL of methanol, 0.407 g ($1.07 \times 10^{-3}$ mol) of 1-pyrenylmethyl 2-bromopropanoate, and 18 mL ($1.07 \times 10^{-1}$ mol) of dimethylaminoethyl methacrylate under a $N_2$ atmosphere. The reaction mixture was degassed by three freeze−pump−thaw cycles, back-filled with $N_2$. After 25 min polymerization at 25 °C, it was cooled with liquid nitrogen, and the contents were diluted in $CH_2Cl_2$. The reaction mixture was then passed through a column of neutral alumina to remove the copper salts. The polymer was precipitated twice from an excess of cold pentane, filtered, and dried at 40 °C under vacuum for 24 h. Monomer conversion and overall yield: 50%. $^1$H NMR ($CDCl_3$) $\delta$ (ppm): 8.3−8 (m, 9H aromatic pyrene), 4.1 (t, 2H, OC$H_2$CH$_2$N(CH$_3$)$_2$), 2.6 (t, 2H, OCH$_2$C$H_2$N(CH$_3$)$_2$), 2.3 (s, 6H, OCH$_2$CH$_2$N(C$H_3$)$_2$), 2.1−1.6 (broad, 2H, aliphatic main chain) 1.3−0.7 (broad, 3H C$H_3$ main chain). SEC: $M_n$ = 10 400 g mol$^{-1}$, $M_w/M_n$ = 1.1 (polystyrene standards). $^1$H NMR using labeled pyrene as reference: $M_n$ = 8500 g mol$^{-1}$.

**Synthesis of Poly(dimethylaminoethyl methacrylate)$_{54}$-*block*-poly(methyl methacrylate$_{55}$-*random*-coumarin methacrylate$_{19}$), PDMAEMA$_{54}$-*b*-P(MMA$_{55}$-*co*-MMA$_{19}$), by ATRP**. CuCl (30.7 mg, $3.1 \times 10^{-4}$ mol), PMDETA (65 $\mu$L, $3.1 \times 10^{-4}$ mol), Py-PDMAEMA (2.6 g, $3.1 \times 10^{-4}$ mol), anisole (26 mL), methyl methacrylate (2.925 mL, $2.71 \times 10^{-2}$ mol), and 7-(2-methacryloyloxyethoxy)-4-methylcoumarin (2.6 g, $9.02 \times 10^{-3}$ mol) were added under a $N_2$ atmosphere into a round-bottom flask that was flamed and dried under vacuum. The reaction mixture was degassed by three freeze−pump−thaw cycles, back-filled with $N_2$, and placed in an oil bath thermostated at 65 °C for 1 h. The resulting copolymer was diluted with dichloromethane and passed through a column of neutral alumina to remove the ATRP catalyst. The polymer was precipitated twice from a mixture of hexane/THF (80/20), filtered, and dried at 40 °C under vacuum for 24 h. Monomers conversion and overall yield: 55%. $^1$H NMR ($CDCl_3$) $\delta$ (ppm): 8.3−8 (m, 9H aromatic pyrene), 7.7−6 (m, 4H aromatic coumarin), 4.5−4.1 (m, 4H C$H_2$C$H_2$O-coumarin), 4.1 (t, 2H, OC$H_2$CH$_2$N(CH$_3$)$_2$), 3.6 (s, 3H COOC$H_3$), 2.6 (t, 2H, OCH$_2$C$H_2$N(CH$_3$)$_2$), 2.3 (s, 6H, OCH$_2$-CH$_2$N(C$H_3$)$_2$), 2.1−1.6 (broad, 2H, aliphatic main chain and C$H_3$ coumarin) 1.3−0.7 (broad, 3H C$H_3$ main chain). SEC (THF): $M_n$ = 22 000 g mol$^{-1}$, $M_w/M_n$ = 1.08.

**Scheme 1. Reaction Pathway for the Synthesis of the Diblock Copolymer of PDMAEMA$_{54}$-*b*-P(MMA$_{55}$-*co*-CMA$_{19}$)**

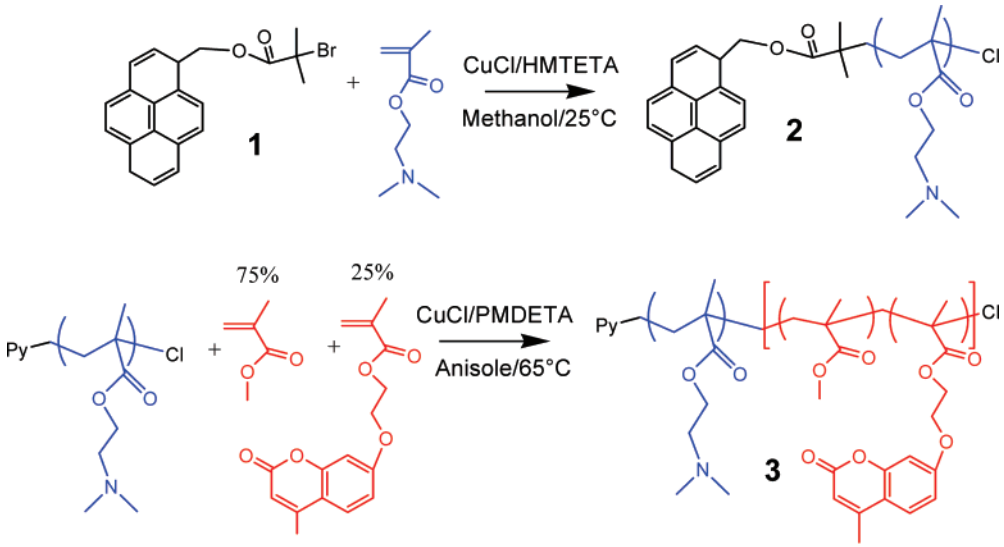


**2. Preparation of Shell Cross-Linked Reverse Micelles (SCRM).** PDMAEMA$_{54}$-*b*-P(MMA$_{55}$-*co*-MMA$_{19}$) (250 mg) was dissolved in dichloromethane (125 mL). A solution of HCl in THF (80 mL, 0.01 M) was then added dropwise under moderate stirring. The whole micellar solution (305 mL) was then exposed to UV light at $\lambda_{max} > 310$ nm for the photo-cross-linking (5 h, 2000 mW). Afterward, 30 mL of DMF was added, and THF/dichloromethane solvents were removed by rotary evaporation. The reason for the solvent exchange is as follows. While SCRM solutions were stable after the cross-linking step, we have noticed that after evaporation of the mixture of solvents (THF/$CH_2Cl_2$) the resulting powder of SCRM could not be solubilized by solvents commonly employed in ATRP processes. Because of the cross-linking, the shell partially lost its capacity to solubilize the dry aggregates. To circumvent this problem, SCRM have been kept always in DMF that was the solvent for SCRM-initiated ATRP. The final concentration of SCRM in DMF was 5.5 mg mL$^{-1}$. DLS (DMF): $D_H = 36.6$ nm. SEC (THF): $M_n = 410\,000$ g mol$^{-1}$, $M_w/M_n = 1.03$. $^1$H NMR ($d_6$-DMSO) $\delta$ (ppm): 3.4 (s, 3H COOC$H_3$).

**3. Grafting of SCRM through Surface-Initiated ATRP. Polymerization of Styrene**. CuCl (4.73 mg, $4.73 \times 10^{-5}$ mol), PMDETA (10 $\mu$L, $4.73 \times 10^{-5}$ mol), SCRM (1.8 mL in DMF, 10 mg, $4.73 \times 10^{-7}$ mol), and styrene (2 mL, $1.74 \times 10^{-2}$ mol) were added under a $N_2$ atmosphere to a round-bottom flask that was flamed and dried under vacuum. The reaction mixture was degassed by three freeze−pump−thaw cycles, back-filled with $N_2$, and placed in an oil bath thermostated at 100 °C for 20 h. Polymerization was monitored using SEC by injecting an aliquot of the reaction mixture at different polymerization times.

**Polymerization of Dimethylaminoethyl Methacrylate**. CuCl (5.6 mg, $5.6 \times 10^{-5}$ mol), HMTETA (15 $\mu$L, $5.6 \times 10^{-5}$ mol), SCRM (2 mL in DMF, 11 mg, $5.65 \times 10^{-7}$ mol), and DMAEMA (2 mL, $2.71 \times 10^{-2}$ mol) were added under a $N_2$ atmosphere to a round-bottom flask that was flamed and dried under vacuum. The reaction mixture was degassed by three freeze−pump−thaw cycles, back-filled with $N_2$, and placed in an oil bath thermostated at 60 °C for 16 h. The reaction mixture was then dialyzed against water (MWCO 50 000 kDa) for 5 days to remove any unreacted monomers and catalysts. Finally, the product was recovered by lyophilization. DLS(water): $D_H = 58$ nm. SEC: $M_n = 730\,000$ g mol$^{-1}$, $M_w/M_n = 1.05$. $^1$H NMR ($d_6$-DMSO/$CDCl_3$; 20/80; v/v) $\delta$ (ppm): 4.1 (t, 2H, OC$H_2$CH$_2$N(CH$_3$)$_2$), 2.6 (t, 2H, OCH$_2$C$H_2$N-(CH$_3$)$_2$), 2.3 (s, 6H, OCH$_2$CH$_2$N(C$H_3$)$_2$), 2.1−1.6 (broad, 2H, aliphatic main chain) 1.3−0.7 (broad, 3H C$H_3$ main chain).

**4. Characterizations.** $^1$H NMR spectra were recorded at room temperature on a Bruker spectrometer (300 MHz, AC 300). UV−vis absorption and fluorescence emission spectra were recorded on the Varian spectrophotometers of Cary 50 and Cary Eclipse, respectively. Size exclusion chromatography (SEC) measurements were performed using a Waters system equipped with a refractive index detector (RI 410), a photodiode array detector (PDA 996), and one column (Styragel 5HE 7.8 mm × 300 mm). The eluent used was dichloromethane with 2% of triethylamine (elution rate, 1 mL min$^{-1}$) at 40 °C. SEC was calibrated using polystyrene standards. Micellar aggregates were examined using a HitachiH-7500 transmission electron microscope (TEM) operating at 80 kV. Samples for TEM were prepared by casting one drop of the micellar solution on a carbon-coated copper grid, followed by drying and, in some cases, negative staining with phosphotungstic acid. The photo-cross-linking procedure was conducted by applying UV light, generated by a UV−vis spot-curing system (Novacure, 320-500 filter, 2 W), vertically from above the cell containing the micellar solution. As for the photo-de-cross-linking, the irradiation light was obtained directly from a UV-C Air sterilizer lamp (1.25 W, $\lambda_{max} =$ 254 nm), placed at about 7 cm away from the sample quartz cell. Dynamic light scattering (DLS) experiments were performed on a Brookhaven goniometer (BI-200) equipped with a highly sensitive avalanche photodiode detector (Brookhaven, BI-APD), a digital correlator (Brookhaven, TurboCorr) that calculates the photon intensity autocorrelation function $g^2(t)$, and a helium−neon laser ($\lambda = 632.8$ nm). The hydrodynamic diameter ($D_H$) and polydispersity (PDI) values of the aggregates were obtained by a cumulant and CONTIN analysis.

## Results and Discussion

**1. Synthesis of PDMAEMA$_{54}$-*b*-P(MMA$_{55}$-*co*-CMA$_{19}$).** The synthetic route to the amphiphilic photoreactive diblock copolymer, from which the shell cross-linked reversed micelles (SCRM) were constructed, is outlined in Scheme 1. We started with the synthesis of the pyrene-based atom transfer radical polymerization (ATRP) initiator, **1**. For this, 2-bromo-2-methylpropionyl bromide was added at 0 °C to 1-methanol−pyrene in the presence of triethylamine (TEA), giving rise to 1-pyrenylmethyl 2-bromopropanoate, **1**, in 93% yield. Poly(dimethylaminoethyl methacrylate)$_{54}$ (PDMAEMA$_{54}$), **2**, was grown through ATRP in methanol at 25 °C, using the pyrene-based initiator and the copper chloride (CuCl)/1,1,4,7,10,10-hexamethyltriethylene tetramine (HMTETA) catalytic system. Under these mild conditions, no transesterification reactions between methanol and dimethylaminoethyl groups were detected by $^1$H NMR (Figure 2a). A good control over the molar mass, polydispersity, and functionality (Table 1) was achieved through the halogen exchange from bromide to chloride. $^1$H NMR signal of pyrene chain end (8.3−8 ppm, Figure 2a) was successfully

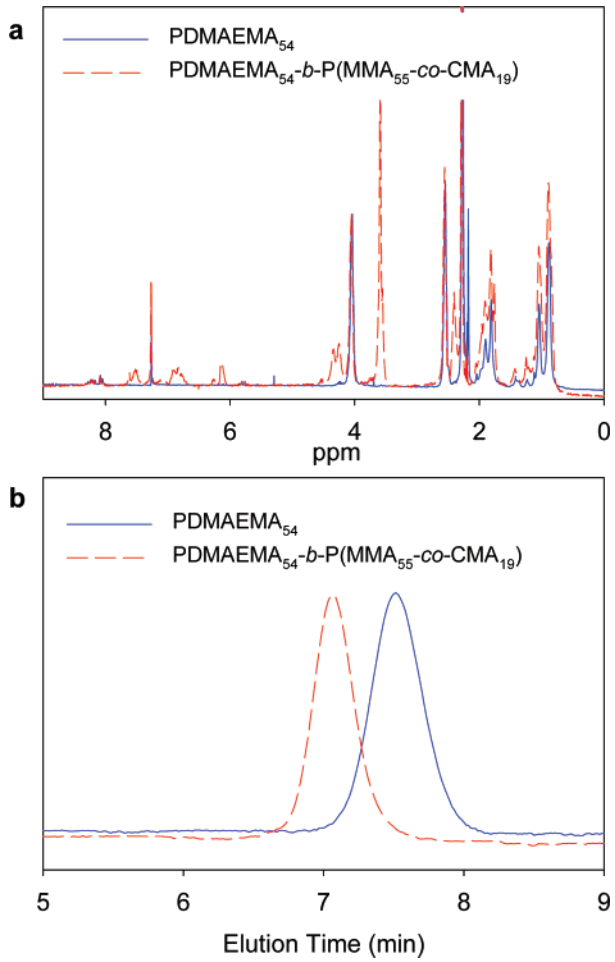


**Figure 2.** (a) $^1$H NMR spectra in $CDCl_3$ and (b) SEC chromatograms of the Py-PDMAEMA$_{54}$ block and the Py-PDMAEMA$_{54}$-*b*-P(MMA$_{55}$-*co*-CMA$_{19}$) block copolymer.

**Table 1. Characteristics of the Macroinitiator, the Diblock Copolymer, and Its Shell Cross-Linked Reverse Micelles (SCRM) before and after the Grafting of Polystyrene and Poly(dimethylaminoethyl methacrylate)**

| sample | $\bar{M}_n{}^a$ (g mol$^{-1}$) | Ip$^a$ | $\bar{M}_n{}^b$ (g mol$^{-1}$) | $D_H^{DLS}$ (nm) | $D^{TEM}$ (nm) |
|---|---|---|---|---|---|
| Py-PDMAEMA$_{54}$ | 10 400 | 1.1 | 8 500 | | |
| Py-PDMAEMA$_{54}$-*b*-P(MMA$_{55}$-*co*-CMA$_{19}$) | 22 000 | 1.08 | 19 500 | | |
| SCRM | 403 000 | 1.03 | | 36 | 30 |
| SCRM-PS-3h | 445 000 | 1.04 | | | |
| SCRM-PS-5h | 497 200 | 1.05 | | | |
| SCRM-PS-20h | 726 000 | 1.08 | | | |
| SCRM-PDMAEMA-16h | 730 000 | 1.05 | | 58 | 50 |

$^a$ Determined by SEC ($CH_2Cl_2$, 1 mL min$^{-1}$, PS standard). $^b$ Determined by $^1$H NMR in $CDCl_3$.

used to estimate the average degree of polymerization of the PDMAEMA$_{54}$ block. The resulting chlorine-terminated macroinitiator, PDMAEMA$_{54}$-Cl, was then used to grow the second block under ATRP conditions, which is a random copolymer of poly(methyl methacrylate)$_{55}$-*co*-poly(coumarin methacrylate)$_{19}$, giving rise to the diblock copolymer of PDMAEMA$_{54}$-*b*-P(MMA$_{55}$-*co*-CMA$_{19}$), **3**. Size exclusion chromatography (SEC) analysis showed a clear shift to a higher molecular weight for the diblock copolymer, in comparison to the Py-PDMAEMA$_{54}$ macroinitiator (Figure 2b). In addition, the total disappearance of the Py-PDMAEMA$_{54}$ signal indicates a quantitative initiation from the macroinitiator, and the narrow molecular weight distribution denotes an excellent control of the polymerization process (Table 1). The composition of the random copolymer block was determined by $^1$H NMR, comparing the intensity of dimethylamino proton peaks at $\delta = 2.3$ ppm for PDMAEMA to the intensity of aromatic proton peaks at $\delta = 7.7-6$ ppm for PCMA and the intensity of methyl proton peaks at $\delta = 3.6$ ppm for PMMA (Figure 2a). The $^1$H NMR-determined composition of the random copolymer block ($DP^{PMMA}/DP^{PCMA} = 2.9$) well matched the initial monomer feed ratio (MMA/CMA = 3). This result indicates a similar reactivity for the two monomers and, thus, confirms the random nature of the P(MMA$_{55}$-*co*-CMA$_{19}$) block.

**2. Preparation of Shell Cross-Linked Reverse Micelles (SCRM).** The preparation of SCRM with active chloride end chains on the micelle surface first involved the preparation of the reverse polymer micelles with the hydrophilic PDMAEMA$_{54}$ block in the core and the hydrophobic photoreactive P(MMA$_{55}$-*co*-CMA$_{19}$) block in the shell. As detailed by Eisenberg and co-workers,[20] block ionomers constituted by a nonionic segment and a shorter ionic block can form very stable reverse micelles when dissolved in organic solvents. For example, they showed that in solvents of low polarity such as THF, DMF, or $CHCl_4$, diblock ionomers composed of a short poly(metal methacrylate) ionic segment and a longer PS chain could form reverse micelles comprising an ionic core surrounded by the soluble PS block.[20] On the basis of these results, the aggregation of the PDMAEMA$_{54}$-*b*-P(MMA$_{55}$-*co*-CMA$_{19}$) diblock copolymer into reverse micelles was induced by slow quaternization of the tertiary amine side groups of the PDMAEMA block by hydrochloric acid (HCl) in a mixture of organic solvents (THF/$CH_2Cl_2$, 1/1; v/v). We successfully used SEC to investigate the formation of the reverse micelles. Figure 3a presents the SEC chromatograms of the PDMAEMA$_{54}$-*b*-P(MMA$_{55}$-*co*-CMA$_{19}$ solutions, with different levels of neutralization of the PDMAEMA segment by varying the amount of HCl. Before SEC injections, all solutions were irradiated at $\lambda_{max} > 310$ nm to dimerize the coumarin functions and thus to stabilize the possible micellar aggregates. Below 30% of neutralization the SEC curves were identical to the nonionic precursor and could be therefore assigned to molecularly dissolved block copolymer chains. With 80% of neutralization, a second peak was observed at lower elution time and was attributed to the reverse micelle. At this neutralization degree, there was coexistence between aggregates and single chains in solution. Finally, at 100% neutralization only the peak at low elution time was present, indicating a complete incorporation of single chains into the reverse micelles. In the latter case, the quantitative analysis of the SEC trace (Table 1) revealed a relatively high apparent molecular weight and a very low polydispersity for the aggregates. The existence of reverse micelles was also confirmed by TEM (Figure 3b). Negative staining with phosphotungstic acid (inversed contrast) revealed the presence of spherical white objects, with an average diameter of 30 nm, surrounded by a more contrasted halo (accumulation of the staining agent). DLS results obtained in DMF (after shell cross-linking) confirmed that the hydrodynamic diameters distribution of the reverse micelles was centered to 36 nm with a polydipersity index of 0.062 (Figure 6c). The average diameter measured by TEM was smaller than that obtained by DLS because the former reflected the state of the reverse micelles in the dry state, for which the P(MMA$_{55}$-*co*-CMA$_{19}$) block collapsed, while the latter reflected the conformation of the aggregates in the wet state with the corona fully solvated.

The stabilization of the reverse micelles via shell cross-linking was then realized to ensure the structural integrity of the

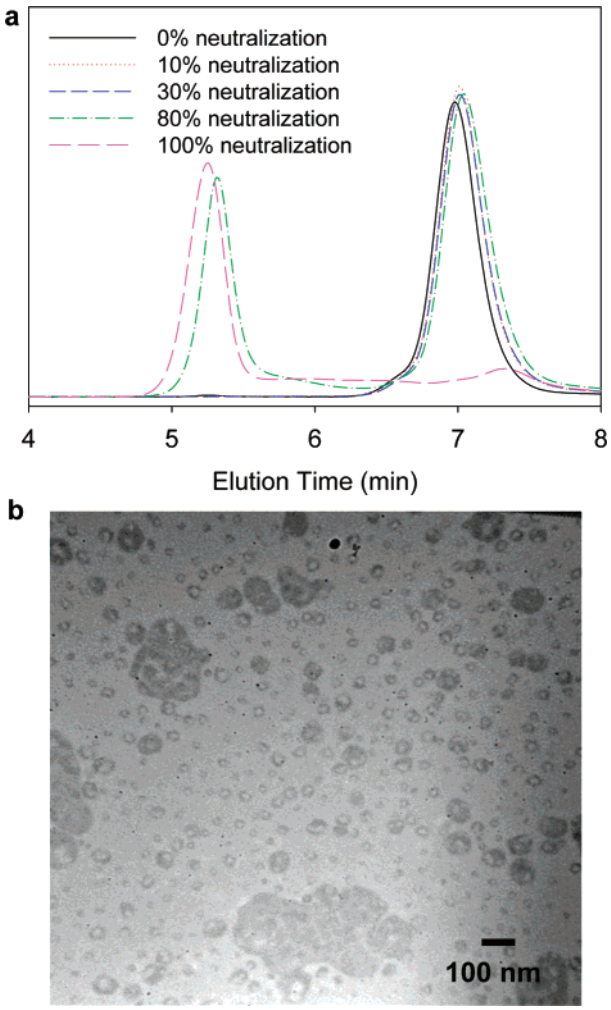


**Figure 3.** (a) SEC chromatograms of PDMAEMA$_{54}$-*b*-P(MMA$_{55}$-*co*-CMA$_{19}$) solutions with different neutralization levels of the PDMAEMA block by HCl. (b) TEM image of the reverse micelles obtained at 100% of neutralization (negatively stained with phosphotungstic acid).

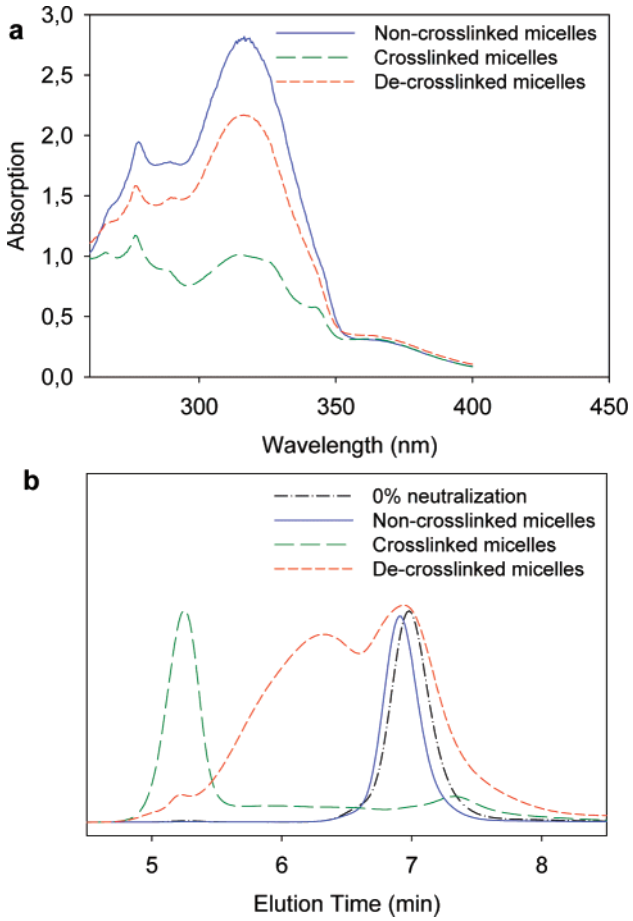


**Figure 4.** (a) UV−vis spectra and (b) SEC chromatograms of reverse micelle solutions before and after the UV irradiation at $\lambda_{max} > 310$ nm for shell cross-linking and after the UV irradiation at $\lambda_{max} < 260$ nm for shell de-cross-linking.

nanoparticles during the postdecoration process using surface-initiated ATRP that took place in critical conditions (elevated temperatures and presence of hydrophilic monomer such as DMAEMA). Recently, we proposed the use of the photoinduced dimerization of coumarin moieties and the photoinduced cleavage of the dimers at two different wavelengths to achieve the stabilization on demand of polymer micelles.[18] In the present study, the diblock copolymer was designed to have a number of coumarin methacrylate units in the hydrophobic block, which allowed us to obtain SCRM by photo-cross-linking (Figure 1). We investigated the stability of our SCRM. Figure 4a shows the UV−vis spectra of the reverse micelles with an ionic core of the completely quaternized PDMAEMA block by HCl, before UV irradiation, after 10 min UV irradiation at $\lambda_{max} = 365$ nm, and after 5 min of subsequent UV irradiation at $\lambda_{max} = 254$ nm. Upon the first UV irradiation, the absorption of coumarin functions at around 320 nm decreased, indicating the occurrence of dimerization and thus the cross-linking of the shell. After the SCRM solution was subsequently illuminated with the second UV light (shorter wavelengths), the opposite process, i.e., photocleavage of cyclobutane bridges[21] (Figure 1), partially took place as indicated by the incomplete but substantial recovery of the UV absorption at 320 nm. As shown in Figure 4b, SEC measurements of these three solutions confirmed the excellent stability of the SCRM. For this SEC experiment, triethylamine was added into the $CH_2Cl_2$ eluent (2% in volume) in order to trap HCl in-situ and thus convert the PDMAEMA block back to the nonionic form. The un-cross-linked reverse micelles were totally dissolved in the eluent and displayed almost the same SEC trace as the molecularly dissolved nonionic diblock copolymer (also shown for comparison). By contrast, SCRM showed only a peak at lower elution time corresponding to the preserved micellar aggregates. This shows the great efficiency of the shell photo-cross-linking in preventing the reverse micelles, with the PDMAEMA core becoming soluble in the eluent, from disintegration. For the SCRM solution subjected to the photo-de-cross-linking, despite the incomplete cleavage of the cyclobutane bridges (cross-linking points), only a very small fraction of SCRM remained intact, displaying the peak at the same short elution time as SCRM. A large portion of the initial SCRM were totally disintegrated showing a peak at longer elution time corresponding to the dissolved nonionic precursor of the diblock copolymer; while the remainder of the initial SCRM were partially disintegrated showing up at intermediate elution times. Therefore, these results clearly show that the photoinduced dimerization of coumarin moieties is effective in locking in the reverse polymer micelles and provides the structural integrity required for the postdecoration of SCRM using surface-initiated ATRP of a selected monomer. Moreover, the results also show that the photocleavage of coumarin dimers at a different wavelength can severely disintegrate the SCRM. This is the first light-controllable reverse polymer micelles, which differ from the light-controllable polymer micelles with a hydrophobic core reported previously by our group[18,22] and others.[23] Its potential use as a nanocarrier for encapsulating

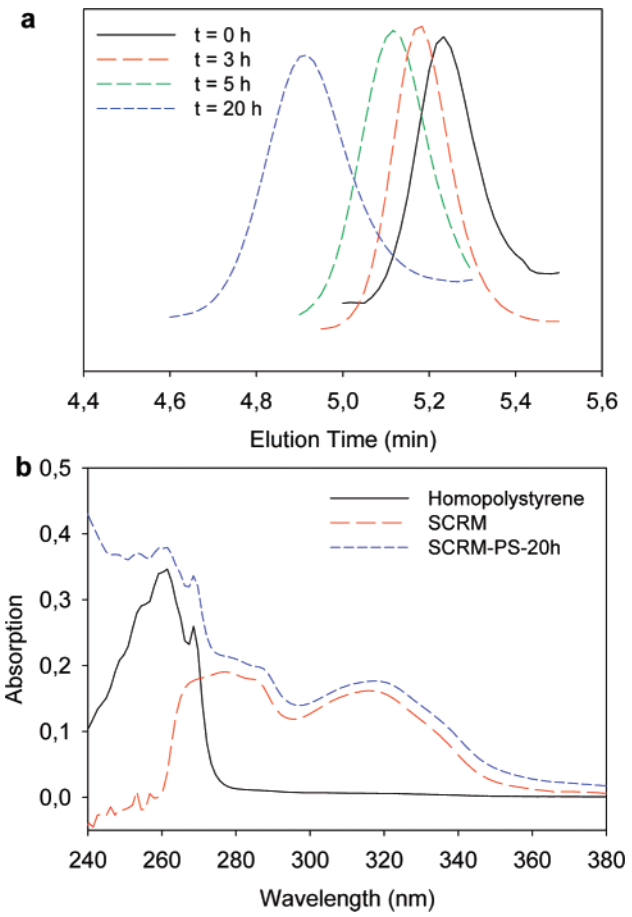


**Figure 5.** (a) SEC chromatograms for different times of styrene polymerization from the surface of SCRM. (b) UV spectra extracted from SEC curves for homopolystyrene, SCRM, and SCRM-PS-20h.

hydrophilic guest molecules and their release controlled by light is the subject of future investigations.

**3. "Decoration" of SCRM through Surface-Initiated ATRP.** Our first attempt to decorate the SCRM surface by ATRP was made using styrene that is a commonly employed monomer. Styrene was polymerized in a DMF solution at 100 °C in the presence of SCRM and the CuCl/*N*,*N*′,*N*′,*N*′′-pentamethyldiethylenetriamine (PMDETA) catalytic system. High dilution condition ($C_{SCRM} \approx 0.3$ wt %) was chosen to minimize the extent of the possible irreversible termination by SCRM−SCRM coupling. Indeed, Gnanou et al. showed with a dendritic-type ATRP initiator that the probability of irreversible coupling between stars increases rapidly with the monomer conversion and that a high initial monomer/initiator ratio (high dilution) has to be applied to avoid alteration of the functionality of the samples.[24,25] With this high dilution condition, a ratio [catalyst]/[initiator] = 100 was utilized to increase the reaction rate and to ensure a good control of the polymerization from active chloride groups exposed on the SCRM surfaces. To monitor the progress of polymerization, aliquots of the reaction mixture were taken using a syringe at timed intervals and directly injected into SEC. Figure 5a shows the SEC curves before and after 3, 5, and 20 h of polymerization. The corresponding number-average molecular weights and polydispersity indices are given in Table 1 (SCRM-PS entries). It can be seen that the peak of SCRM ($t$ = 0 h) was shifted progressively to shorter elution time with increasing the polymerization time. This indicates an increase in size of SCRM that logically should come from the SCRM surface-initiated ATRP of styrene. After 20 h of reaction, the apparent molecular weight increased from 403 000 to 726 000 g mol$^{-1}$ with a relatively constant low polydispersity index. These results suggest a successful growth of PS chains from the surface of SCRM. The fact that the elution peaks after polymerization remained sharp and symmetrical and showed no tailing at higher and lower elution time indicates a good control of the ATRP from the SCRM initiator, a high initiating efficiency, and the absence of coupling reactions between the micellar aggregates. To further confirm the presence of PS on the surface of SCRM, UV−vis spectra were extracted from the SEC curves at the elution peak using the photodiode array detector; Figure 5b presents the spectra obtained for SCRM (before polymerization), SCRM-PS-20h (20 h after polymerization), and a PS homopolymer sample for the sake of comparison. While the spectrum of SCRM only shows the dimerized coumarin signal (280 nm < $\lambda$ < 360 nm), both the signals of dimerized coumarin and PS (240 nm < $\lambda$ < 280 nm) can be noticed for SCRM-PS-20h. This indicates the presence of PS chains at the elution time of the aggregates, further confirming the polymerization of styrene from the surface of SCRM. However, more detailed analysis using $^1$H NMR spectroscopy or DLS could not be performed due to the presence of PS homopolymer in the solution, which appeared at longer elution time on the SEC curves (not shown). This was probably caused by some thermally initiated polymerization of styrene as the reaction was carried out at 100 °C for 20 h.

The first test of the strategy using the monomer of styrene thus confirmed the effective ATRP initiated by the chloride groups on the surface of SCRM. On the basis of those results, we used the SCRM to polymerize dimethylaminoethyl methacrylate (DMAEMA), i.e., the same monomer as that for the hydrophilic polymer constituting the core of SCRM. The purpose was to demonstrate the construction of a new stimuli-responsive nanostructure that cannot be obtained through direct block copolymer self-assembly. The same ATRP conditions as for styrene were applied, only with the reaction temperature reduced to 60 °C (instead of 100 °C) in order to minimize the thermally initiated polymerization and the 1,1,4,7,10,10-hexamethyltriethylenetetramine (HMTETA) ligand used to replace PMDETA. After 16 h of polymerization, the sample (SCRM-PDMAEMA-16h) was dialyzed against water for 5 days to remove any unreacted monomers and most of the catalytic complex and was recovered by lyophilization. The obtained powder was characterized by SEC, $^1$H NMR, DLS, and TEM; all the results (Figure 6 and Table 1) show the successful grafting of PDMAEMA onto the surface of SCRM. SEC curves (Figure 6a) revealed an increase of the average molecular weight from 406 000 to 730 000 g mol$^{-1}$ and the preservation of a very low polydipersity for the resulting larger aggregates, indicating the absence of coupling reactions between them as well as the absence of PDMAEMA homopolymer. $^1$H NMR spectra recorded before and after the polymerization (Figure 6b) clearly showed the appearance of the characteristic peaks of PDMAEMA for SCRM-PDMAEMA-16h, while mainly the methyl peak of PMMA units at $\delta$ (ppm) = 3.4 was prominent in the spectrum of SCRM due to the insolubility of dimerized coumarin moieties and the PDMAEMA located respectively in the shell and in the core of SCRM. Moreover, DLS measurements confirmed a significant increase of the hydrodynamic diameter from 36 nm for SCRM to 58 nm for SCRM-PDMAEMA-16h (Figure 6c). Finally, direct observation of the SCRM-PDMAEMA-16h aggregates by TEM (without negative staining in this case) also revealed the increase in the average size after polymerization (Figure 6d) from 30 ± 10 to 50 ± 15 nm. The highly contrasted small objects ($D$ < 10 nm) on the TEM image

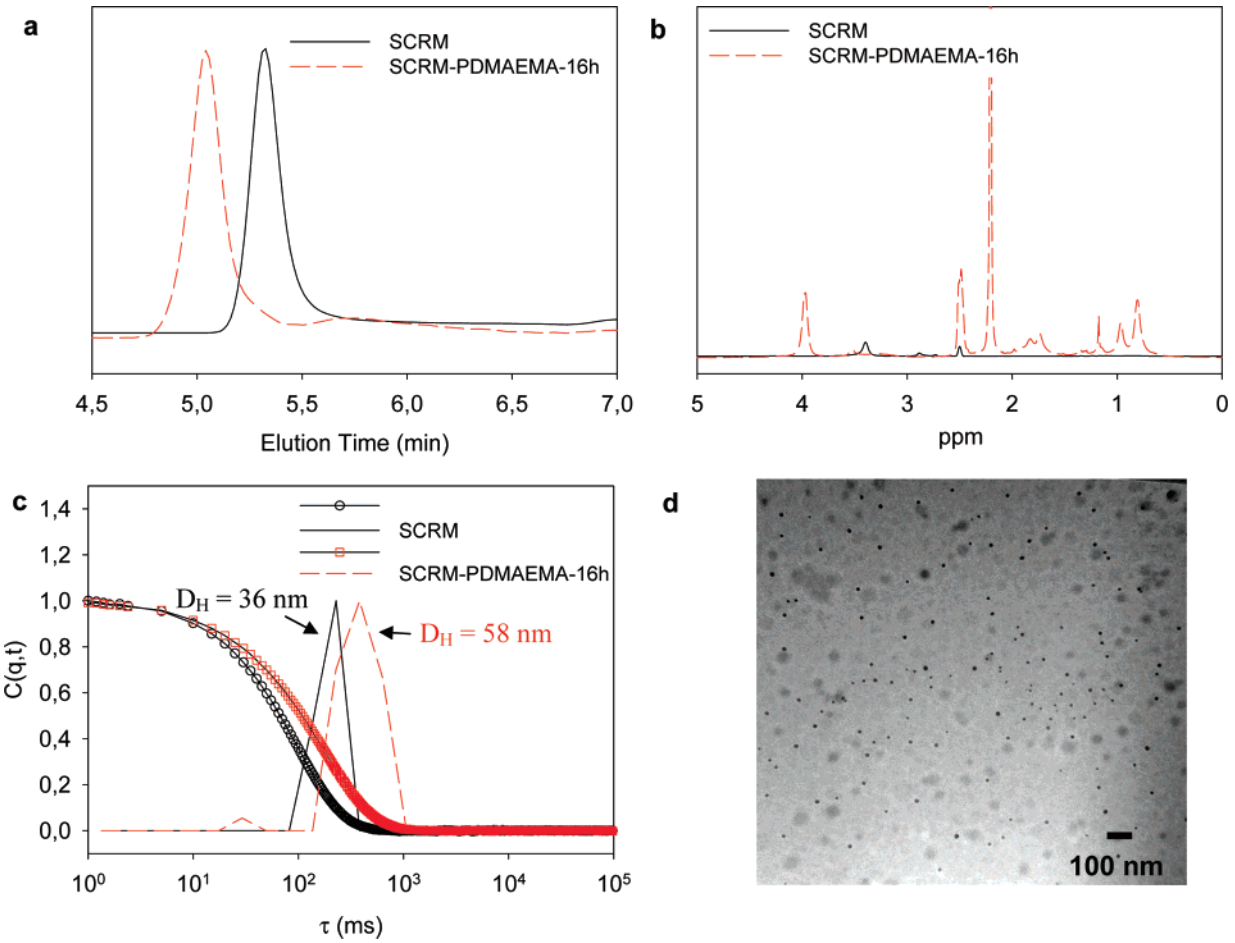


**Figure 6.** (a) SEC chromatograms, (b) $^1$H NMR spectra (SCRM: $d_6$-DMSO; SCRM-PDMAEMA-16h: $d_6$-DMSO/$CDCl_3$; 20/80; v/v), (c) autocorrelation functions and relaxation time distribution (CONTIN), and (d) TEM image for the nanoparticles before (SCRM) and after polymerization of DMAEMA from surface (SCRM-PDMAEMA-16h). The TEM image of SCRM is shown in Figure 3b.

were assigned to the residue of CuCl. Assuming that PDMAEMA chains on surface were fully extended (they are highly protonated in water at pH 7 as the p$K_a$ of PDMAEMA is about 8.4[26−28]), we could roughly estimate the number of PDMAEMA segments present on the surface of SCRM according to

$$N = 2L_{\mathrm{DMAEMA}}(M_{\mathrm{n,SEC}}^{\mathrm{SCRM-PDMAEMA-16h}} - M_{\mathrm{n,SEC}}^{\mathrm{SCRM}})/(D_{\mathrm{H}}^{\mathrm{SCRM-PDMAEMA-16h}} - D_{\mathrm{H}}^{\mathrm{SCRM}})M_{\mathrm{DMAEMA}}$$

Using $L_{\mathrm{DMAEMA}} = 0.25$ nm (length of monomeric unit) and $M_{\mathrm{DMAEMA}} = 157$ g mol$^{-1}$ (monomer molar mass) yields $N \approx 47$. This number, though very approximative, indicates an effective growth of PDMAEMA chains through SCRM surface-initiated ATRP.

The decorated SCRM are thus nanoparticles constituted of a dense hydrophilic inner core of $PDMAEMA_{54}$, surrounded by a hydrophobic cross-linked layer of P($MMA_{55}$-*co*-$CMA_{19}$), and an outer hydrophilic corona of PDMAEMA. Even with the assumption that the increase in $D_H$ from 36 to 58 nm was due to fully extended PDMAEMA chains on the SCRM surface, the average degree of polymerization of the grafts would be larger than 54, which is the number of DMAEMA units forming the inner core of the nanoparticles. Such morphology, with two groups of chain lengths of the same polymer located in the inner core and the outer corona respectively, could not be obtained by direct self-assembly of block copolymers. Another obvious interest is that the same SCRM can easily be decorated with a variety of polymers with tunable chain length and functionalities, without the need for different syntheses of block copolymers. Moreover, the grafting of PDMAEMA onto SCRM also made the nanoparticles stimuli-responsive, as evidenced by their reversibly changing solubility in water in response to changes in temperature and pH (Figure 7). While undecorated SCRM is not soluble in water (brown deposit, image a), SCRM-PDMAEMA-16h nanoparticles are fully soluble at pH 7 and 25 °C due to the presence of water-soluble PDMAEMA on the surface (brown solution image b). At pH 7 and 55 °C the solution of SCRM-PDMAEMA-16h become turbid (image c). It is well-known that the PDMAEMA homopolymer undergoes a thermal phase transition in water above its lower critical solution temperature (LCST) of 32−52 °C.[26−29] At temperatures below the LCST, the PDMAEMA chains are water-soluble due to the predominantly intermolecular hydrogen-bonding interactions between DMAEMA units and water, whereas at temperature above the LCST, intramolecular hydrogen-bonding interactions between DMAEMA units become predominant, inducing the collapse of the polymer chains. Therefore, at 55 °C PDMAEMA chains on the surface of SCRM became insoluble in water which induced the precipitation of the aggregates (image c). Finally, keeping the temperature at 25 °C but raising the pH to 12, the SCRM-PDMAEMA-16h nanoparticles also became insoluble in water (image d). Indeed, PDMAEMA is a weak polybase that is soluble in water at low pH and insoluble at high pH when totally deprotonated.[30] All theses changes in solubility are reversible.

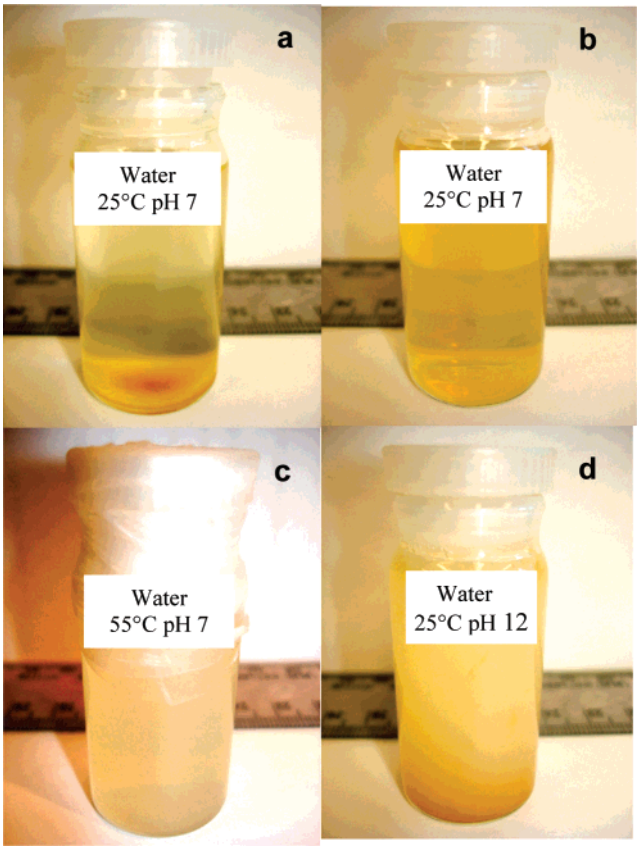


**Figure 7.** Digital photographs of the aqueous solutions of (a) SCRM at 25 °C and pH 7; (b) SCRM-PDMAEMA-16h at 25 °C and pH 7; (c) SCRM-PDMAEMA-16h at 55 °C and pH 7; and (d) SCRM-PDMAEMA-16h at 25 °C and pH 12.

## Conclusions

We presented a new approach to prepare stimuli-responsive polymer nanoparticles that combines block copolymer self-assembly and postfunctionalization using surface-initiated ATRP. We designed and synthesized the new diblock copolymer of PDMAEMA$_{54}$-*b*-P(MMA$_{55}$-*co*-CMA$_{19}$), whose reverse micelles with the ionic PDMAEMA$_{54}$ core can be stabilized through photoinduced cross-linking of the hydrophobic shell of P(MMA$_{55}$-*co*-CMA$_{19}$). The chloride groups preserved on the surface of such structurally locked shell cross-linked reverse micelles (SRCM) allow for well-controlled growth of another polymer such as PDMAEMA through ATRP, resulting in monodispersed polymer nanoparticles that differ from those formed by block copolymer self-assembly. The grafting of the hydrophilic PDMAEMA chains renders the SCRM soluble in water at pH 7 and room temperature, with the solubility being sensitive to changes in pH and temperature. In addition, the new nanoparticles are light-responsive. As the shell cross-linking is made possible with the photoinduced reversible dimerization of the coumarin moieties on the P(MMA$_{55}$-*co*-CMA$_{19}$) block ($\lambda > 310$ nm), it is possible to de-cross-link the shell with the photocleavage of the cyclobutane bridges upon UV irradiation ($\lambda < 260$ nm), which results in the disintegration of SCRM.

**Acknowledgment.** We acknowledge the financial support from The Cancer Research Society Inc. (Canada) for this work. We also thank Drs. Jinqiang Jiang and Bo Qi for their help at the early stage of this work. Y.Z. is a member of the FQRNT-funded Center for Self-Assembled Chemical Structures. M.L. is a member of the FRSQ-funded Centre de recherche clinique Étienne-Le Bel and is the Canada Research Chair in Magnetic Resonance Imaging.

## References and Notes

(1) Mattyjaszewski, K.; Xia, J. *Chem. Rev.* **2001**, *101*, 2921.
(2) Radhakrishnan, B.; Ranjan, R.; Brittain, W. J. *Soft Matter* **2006**, *2*, 386.
(3) Chen, X.; Randall, D. P.; Perruchot, C.; Watts, J. F.; Patten, T. E.; von Werne, T.; Armes, S. P. *J. Colloid Interface Sci.* **2003**, *257*, 56.
(4) Mori, H.; Seng, D. C.; Zhang, M.; Muller, A H. E. *Langmuir* **2002**, *18*, 3682.
(5) Pyun, J.; Mattyjaszewski, K.; Kowalewski, T.; Savin, D.; Patterson, G.; Kickelbick, G.; Suesing, N. *J. Am. Chem. Soc.* **2001**, *123*, 9445.
(6) Li, D.; Jones, G. L.; Dunlap, J. R.; Hua, F.; Zhao, B. *Langmuir* **2006**, *22*, 3344.
(7) Angot, S.; Taton, D.; Gnanou, Y. *Macromolecules* **2000**, *33*, 5418.
(8) Couet, J.; Biesalski, M. *Macromolecules* **2006**, *39*, 7258.
(9) Fulghum, T. M.; Patton, D. L.; Advincula, R. C. *Langmuir* **2006**, *22*, 8397.
(10) Rodriguez-Hernandez, J.; Chécot, F.; Gnanou, Y.; Lecommandoux, S. *Prog. Polym. Sci.* **2005**, *30*, 691.
(11) See a recent review: Read, E. S.; Armes, S. P. *Chem. Commun.* **2007**, 3021.
(12) Thurmond II, K. B.; Kowalewski., T.; Wooley, K. L. *J. Am. Chem. Soc.* **1996**, *118*, 7239.
(13) Huang, H.; Kowalewski, T.; Remsen, E. E.; Gertzmann, R.; Wooley, K. L. *J. Am. Chem. Soc.* **1997**, *119*, 11653.
(14) Guo, A.; Liu, G.; Tao, J. *Macromolecules* **1996**, *289*, 2487.
(15) Ding, J.; Liu, G. *Macromolecules* **1998**, *31*, 6554.
(16) Kakizawa.; Y.; Harada, A.; Kataoka, K. *J. Am. Chem. Soc.* **1999**, *121*, 11247.
(17) Li, Y.; Lokitz, B. S.; Armes, S. P.; McCormick, C. L. *Macromolecules* **2006**, *39*, 2726.
(18) Jiang, J.; Qi, B.; Lepage, M.; Zhao, Y. *Macromolecules* **2007**, *40*, 790.
(19) Jones, M.-C.; Tewari, T.; Blei, C.; Hales, K.; Pochan, D. J.; Leroux, J.-C. *J. Am. Chem. Soc.* **2006**, *128*, 14600.
(20) (a) Desjardins, A.; Eisenberg, A. *Macromolecules* **1991**, *24*, 5779. (b) Desjardins, A.; van de Ven, T. G. M.; Eisenberg, A. *Macromolecules* **1992**, *25*, 2412. (c) Zhong, X. F.; Varshney, S. K.; Eisenberg, A. *Macromolecules* **1992**, *25*, 7160.
(21) Hammond, G. S.; Stout, C. A.; Lamola, A. A. *J. Am. Chem. Soc.* **1964**, *86*, 3103.
(22) (a) Wang, G.; Tong, X.; Zhao, Y. *Macromolecules* **2004**, *37*, 8911. (b) Tong, X.; Wang, G.; Soldera, A.; Zhao, Y. *J. Phys. Chem. B* **2005**, *109*, 20281. (c) Jiang, J.; Tong, X.; Zhao, Y. *J. Am. Chem. Soc.* **2005**, *127*, 8290. (d) Jiang, J.; Tong, X.; Morris, D.; Zhao, Y. *Macromolecules* **2006**, *39*, 4633. (e) Zhao, Y. *Chem. Rec.* **2007**, *7*, 286.
(23) (a) Liu, X.; Jiang, M. *Angew. Chem., Int. Ed.* **2006**, *45*, 3846. (b) Lee, H.; Wu, W.; Oh, J. K.; Mueller, L.; Sherwood, G.; Peteanu, L.; Kowalewski, T.; Matyjaszewski, K. *Angew. Chem., Int. Ed.* **2007**, *46*, 2453.
(24) Angot, S.; Murthy, K. S.; Taton, D.; Gnanou, Y. *Macromolecules* **1998**, *31*, 7218.
(25) Lepoittevin, B.; Matmour, R.; Francis, R.; Taton, D.; Gnanou, Y. *Macromolecules* **2005**, *38*, 3120.
(26) Butun, V.; Billingham, N. C.; Armes, S. P. *Chem. Commun.* **1997**, *7*, 671.
(27) Butun, V.; Armes, S. P.; Billingham, N. C. *Polymer* **2001**, *42*, 5993.
(28) Vamvakaki, M.; Unali, G. F.; Bueten, V.; Boucher, S.; Robinson, K. L.; Billingham, N. C.; Armes, S. P. *Macromolecules* **2001**, *34*, 6839.
(29) Gohy, J.-F.; Antoun, S.; Jerome, R. *Macromolecules* **2001**, *34*, 7435.
(30) Bütün, V.; Lowe, A. B.; Billingham, N. C.; Armes, S. P. *J. Am. Chem. Soc.* **1999**, *121*, 4288.

MA702422Y